Available online at www.sciencedirect.com
SCIENCE DIRECT®
Pergamon
Cement and Concrete Research 34 (2004) 249–254
CEMENT AND CONCRETE RESEARCH

Durable fiber reinforced self-compacting concrete

V. Corinaldesi, G. Moriconi*

Department of Materials and Environment Engineering and Physics, Marche Polytechnical University, Via Brecce Bianche, 60131 Ancona, Italy

Received 18 December 2002; accepted 28 July 2003

Abstract

In order to produce thin precast elements, a self-compacting concrete was prepared. When manufacturing these elements, homogenously dispersed steel fibers instead of ordinary steel-reinforcing mesh were added to the concrete mixture at a dosage of 10% by mass of cement. An adequate concrete strength class was achieved with a water to cement ratio of 0.40. Compression and flexure tests were carried out to assess the safety of these thin concrete elements. Moreover, serviceability aspects were taken into consideration. Firstly, drying shrinkage tests were carried out in order to evaluate the contribution of steel fibers in counteracting the high concrete strains due to a low aggregate–cement ratio. Secondly, the resistance to freezing and thawing cycles was investigated on concrete specimens in some cases superficially treated with a hydrophobic agent. Lastly, both carbonation and chloride penetration tests were carried out to assess durability behavior of this concrete mixture.

Keywords: Durability; Fiber reinforcement; Self-compacting concrete

1. Introduction

Self-compacting concrete is considered a concrete that can be placed and compacted under its own weight without any vibration effort, assuring complete filling of formworks even when access is hindered by narrow gaps between reinforcement bars. Concrete that must not be vibrated is a challenge to the building industry. In order to achieve such behavior, the fresh concrete must show both high fluidity and good cohesiveness at the same time. As already outlined by Collepardi [1], some concretes bearing these requirements were first studied in 1975–1976. At that time, neither the modern acrylic-based superplasticizers nor the new viscosity-modifying agents (VMAs) were available. Nevertheless, the simultaneous use of melamine or naphthalene-based superplasticizers with a relatively high content of powdered materials proved to be very effective [2]. The present work steams from that experience and aims at evaluating the durability of this material. A self-compacting concrete was designed for thin precast elements, which only require steel reinforcement for dead and minor loads. For this reason, the addition of steel fibers to the mixture in order to counteract drying shrinkage of concrete was also chosen. However, from a functional point of view, a compressive strength class of 40 MPa was requested, taking into account early flexural strength for lifting and moving, as well as fatigue and creep effects.

2. Concrete preparation

2.1. Materials

A portland–limestone blended cement, type CEM II/A-L 42.5 R according to the European Standards EN-197/1, was used. Its Blaine fineness was 0.363 m^2/g and its specific gravity was 3050 kg/m^3. The chemical composition of the cement is reported in Table 1. A commercial limestone powder, originating from marble, was used as a mineral admixture. It was chosen bearing in mind the suggestion on fineness reported in Ref. [3]; its Blaine fineness was 0.610 m^2/g. Moreover, its specific gravity was 2650 kg/m^3 and its chemical composition is reported in Table 1. Crushed limestone aggregate (10-mm

* Corresponding author. Tel.: +39-071-2204725; fax: +39-071-2204729.
E-mail address: moriconi@univpm.it (G. Moriconi).

0008-8846/$ – see front matter © 2003 Elsevier Ltd. All rights reserved.
doi:10.1016/j.cemconres.2003.07.005

Table 1
Chemical composition of cement and limestone powder

Oxide (%)	Cement	Limestone powder
SiO_2	29.67	38.70
Al_2O_3	3.74	8.02
Fe_2O_3	1.80	3.34
TiO_2	0.09	0.12
CaO	59.25	40.61
MgO	1.15	2.93
SO_3	3.25	1.20
K_2O	0.79	1.37
Na_2O	0.26	1.00
LOI	11.62	34.23

LOI = loss on ignition at 1000 °C.

maximum size) and natural sand (6-mm maximum size) were used. The gradation of both crushed aggregate and sand are shown in Fig. 1, and their physical properties are reported in Table 2. A 40% aqueous solution of a melamine-based polymer was added to the mixture in order to guarantee very high workability. Straight steel fibers, with length and diameter of 11.0 and 0.4 mm, respectively, thus implying an aspect ratio (AR) equal to 28, were employed at a dosage of 0.6% by volume. This dosage was decided on the basis of some information reported in the literature [4–6], and carrying out preliminary tests, which confirmed that an increase in fiber content from 0.5% to 1%, results in lower concrete performance. Finally, a commercial product based on siloxanic resins was used to make the concrete surface hydrophobic.

2.2. Mixture proportions

The mixture proportions of the self-compacting concrete are reported in Table 3, whereas its composition, expressed by volume percentage, is reported in Table 4. With respect to a common concrete (“Ref-0.40” in Table 4), with the same water to cement ratio (0.40) and the same maximum size of aggregate particles (10 mm), a higher content of very fine material (cement and

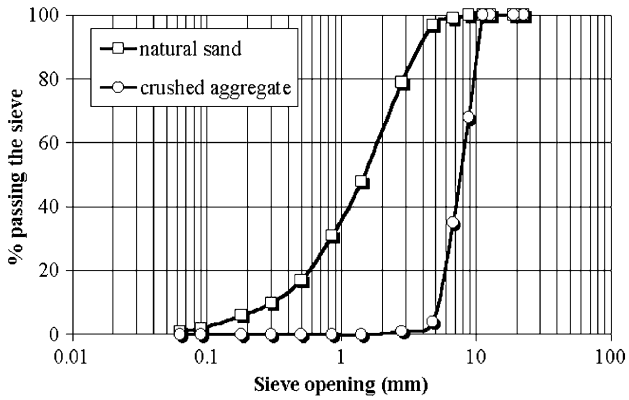

Fig. 1. Grain size distribution curves of the aggregate fractions.

Table 2
Physical properties of the aggregate fractions

Aggregate fractions	Specific gravity (kg/m^3)	Water absorption (%)	Fraction passing 75-μm sieve (%)
Natural sand	2470	1.1	1.0
Crushed aggregate	2710	0.7	0.0

mineral additions) and a lower content of gravel (fraction with grain size higher than 5 mm) had to be used for self-compacting concretes. The exceeding paste is necessary to minimize energy loss caused by coarse particle collisions during concrete flowing through narrow sections [7], and to counteract segregation when the concrete is already placed. The water–cement ratio chosen was equal to 0.40, and the water–fine material ratio was 0.34 due to the addition of limestone powder at a dosage of 16% by mass of cement. In this work, VMAs were not employed; therefore, a very high content of materials passing through ASTM n°100 sieve of 150 μm was necessary [8], up to 19% by volume of concrete (see Table 4). Other conditions that should be respected in order to meet the self-compactibility requirement concern the water–fine material ratio and the sand to mortar ratio; in this work, they were equal to 1.08 and 0.50, respectively, both expressed by volume percentage (see Table 4). In order to obtain a workability measured as high slump flow, a dosage of 1.6% by mass of cement of a melamine-based superplasticizer was necessary.

3. Experimental program and discussion of results

3.1. Slump flow test

As a first step, the properties of the fresh concrete other than slump were evaluated, since in this case the slump value is not relevant being the concrete very fluid. Therefore, the attention was focused on the measurement of the slump flow, which is the mean diameter (Φ_{fin}) of the “cake” of concrete obtained after releasing of a standard slump cone. Then, the elapsed time to gain the mean diameter of

Table 3
Concrete mixture proportions

Water/cement	0.40
Water/fine material	0.34
Aggregate/cement	3

Ingredients	Mixture proportions (kg/m^3)
Water	200
Cement	500
Limestone powder	80
Natural sand	1080
Crushed aggregate	420
Steel fibers	50
Superplasticizer	9.4

Table 4
Concrete composition by volume percentage (%)

	Ref-0.40	SCC-0.40
Water	19.1	20.6
Fine material[a]	15.6	19.1
Sand[b]	20.6	40.9
Gravel[c]	41.1	15.0
Steel fibers	–	0.6
Superplasticizer	0.6	0.9
Air	3.0	2.9

[a] All materials passing through ASTM n°100 sieve of 150 μm.
[b] All materials that can pass the sieve opening of 5 mm, keeping into account that almost 10% of crushed aggregate passes this sieve opening, as observable in Fig. 1.
[c] All materials that cannot pass the sieve opening of 5 mm.

500 mm (t_{500}) and the elapsed time to gain the final configuration (t_{fin}) were also recorded. The results obtained are reported in Table 5. The presence of a halo of cement paste around the cake was not observed. The concrete had enough deformability under its own weight (strictly related to the Φ_{fin} value), and had quite a high viscosity (related to the t_{fin} value), which is necessary to avoid segregation of coarse aggregate particles.

3.2. L-box test

The ability of the concrete of compacting itself under its own weight was evaluated by means of the L-box with horizontal steel bars. Both the difference in the concrete level, between the beginning and the end of the box (ΔH_{fin}), and the elapsed time to establish the final configuration (t_{fin}) were detected. The results obtained are reported in Table 5. The concrete showed satisfactory, but not excellent, results in terms of mobility in narrow sections; in fact, the difference in the concrete level between the beginning and the end of the box was significantly higher than the maximum required, equal to about 30 mm. Nevertheless, for producing the thin precast elements, this workability level resulted adequate, due to the absence of reinforcing steel bars inside the formwork.

3.3. Compression and flexure tests

Cubic specimens, 100 mm in size, and prismatic specimens ($100 \times 100 \times 500$ mm) were manufactured according to Italian Standards UNI 6130-72 for compression and bending tests, respectively; these specimens were cast in stainless steel forms and wet cured at 20 °C. Compression tests according to Italian Standards UNI 6132-72 were carried out on cubic specimens, which were tested at right angles to the casting position. The specimens were loaded at a constant strain rate until failure. Due to the lack of an Italian standard test for measuring direct tension in concrete, it was preferred to measure the tensile strength of concrete by subjecting the concrete beam ($100 \times 100 \times 500$ mm) to flexure with a span of 400 mm (according to B.S. 1881:1970 prescriptions). The maximum tensile stress reached at the bottom of the middle cross section of the tested specimen; in other words, the "Modulus of Rupture" (MOR) was also evaluated. At different curing times (1, 3, 7, 28 and 180 days), three specimens were used for each mechanical test, according to Italian Standards. Fig. 2 shows both compressive and flexural strengths as a function of curing time up to 180 days. The requested compressive strength level of 40 MPa, at 28 days of curing, was easily achieved. Concerning the flexural strength, the contribution of the steel fibers did not appear to be evident, due to the low dosage of fibers employed. No ductility measurement was carried out.

Table 5
Fresh concrete workability: results of slump flow and L-box tests

Slump flow	Slump (mm)	290
	Φ_{fin} (mm)	650
	t_{500} (s)	2
	t_{fin} (s)	30
L-box	ΔH_{fin} (mm)	90
	t_{fin} (s)	30

3.4. Drying shrinkage test

Prismatic specimens ($100 \times 100 \times 500$ mm) were prepared according to Italian Standard UNI 6555-73 "Hydraulic Shrinkage Determination". After 1 day of wet curing, the specimens were stored at constant temperature (20 ± 2 °C) and constant relative humidity ($50 \pm 2\%$) while measuring drying shrinkage at different curing times. Fig. 3 shows the results obtained up to 180 days. A drying shrinkage of 500 μm/m can be predicted after 1 year of exposure to a relative humidity of about 50%. The effectiveness of steel fibers addition in counteracting drying shrinkage of concrete becomes evident because for a concrete with the same mixture composition without

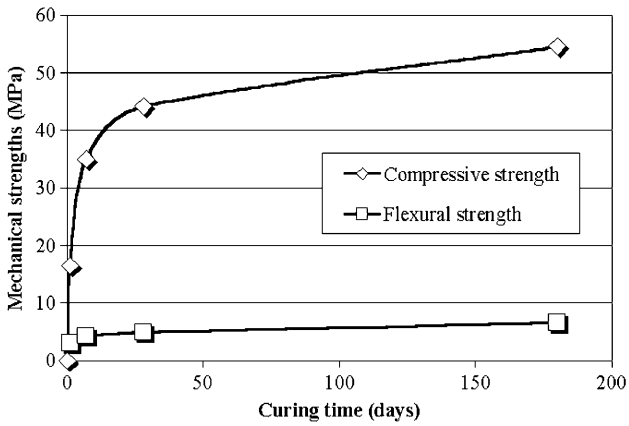

Fig. 2. Compressive and flexural strengths of the concrete as a function of curing time.

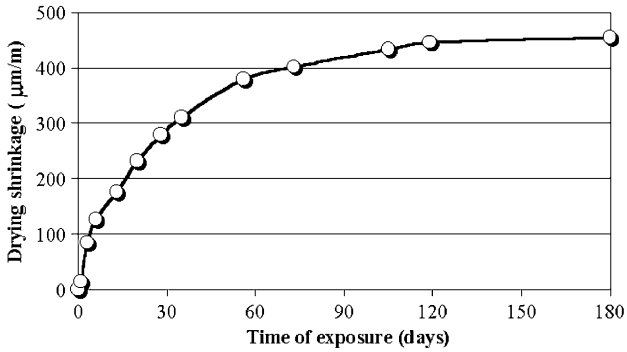

Fig. 3. Drying shrinkage measurements up to 180 days of exposure to 50% relative humidity.

fibers, a drying shrinkage of about 800 μm/m after 6 months can be expected on the basis of well-consolidated data by Lea [9]. Moreover, this result is further confirmed by other researchers independently of the kind of concrete, such as lightweight or fly ash or recycled aggregate and so on, as reported in the literature [10–13].

3.5. Carbonation and chloride penetration depths

The carbonation depth was measured by the phenolphthalein test (RILEM CPC—18) on cubic concrete specimens, 100 mm in size, exposed to air at a temperature of 20 °C after demoulding for 1 day. No carbonation was detected up to 6 months of exposure to air. Fig. 4 shows the chloride penetration depth as a function of the time of exposure to a 10% sodium chloride aqueous solution after water saturation of concrete specimens. Data are reported after 1-month immersion, when instability phenomena due to chloride interference with the cement matrix [14] can be considered over. The chloride penetration into concrete was evaluated through the silver nitrate and fluorescein test [15] on cubic concrete specimens, 100 mm in size, exposed to a 10% sodium chloride aqueous solution after a wet curing of 1 week and an air curing of 3 weeks at a temperature of 20 °C. Both solutions were sprayed on the two fractured surfaces obtained by splitting concrete specimens. Collepardi et al. [15] found that chloride penetration depth (x) varies with the elapsed time (t), following equation obtainable from the solution of Fick's second law under unsteady-state conditions for diffusion in a semi-infinite solid:

$$x = 4 \cdot \sqrt{D \cdot t}$$

where D is the diffusion coefficient of chloride ions into the concrete pores filled with water, expressed in 10^{-8} cm^2/s. The value of D, obtained from the equation by interpolating the results showed in Fig. 4, is $0.25 \cdot 10^{-8}$ cm^2/s at a temperature of about 10 °C. Fig. 5 shows two images obtained by scanning electron microscopy observations on concrete samples after 130 days of immersion in the sodium chloride solution. In the first case (a), the selected region is located 2 mm away from the external surface of the specimen in direct contact with the aggressive solution, whereas in the second case (b), it is placed 30 mm from its edge, and consequently, the steel fiber no longer comes into contact with chloride ions. As a matter of fact, from a morphology point of view, there is slight evidence of corrosion in (a), while a sound fiber shape is detectable in (b).

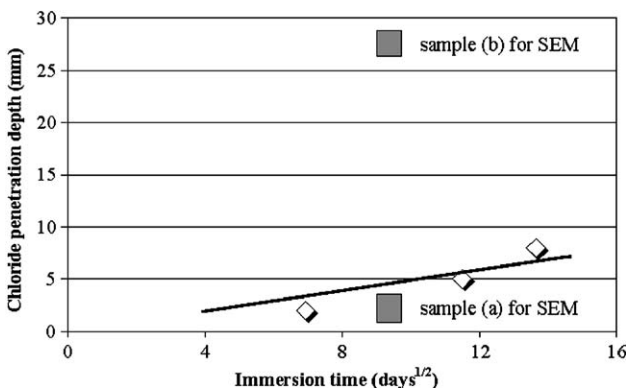

Fig. 4. Chloride penetration as a function of the time of exposure to a 10% sodium chloride aqueous solution.

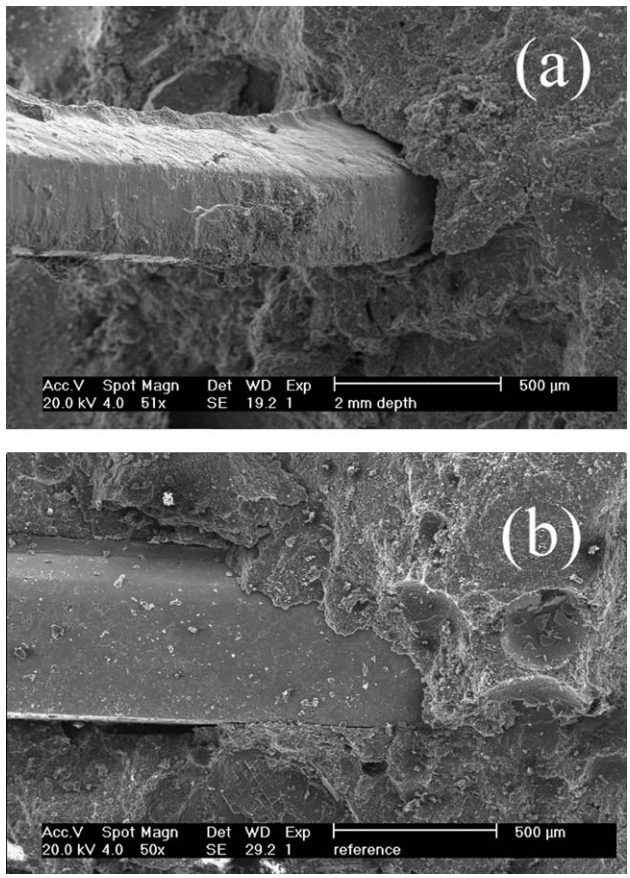

Fig. 5. Images of a fiber located at only 2 mm from the outer surface of a specimen exposed for 130 days to a 10% sodium chloride solution (a) and of a fiber located 30 mm inside the same specimen (b), both obtained by scanning electron microscopy at a magnification of 50×.

Table 6
Pore size distribution of the self-compacting concrete after 90 days of wet curing

Pore diameter (nm)	Porosity (% by volume)
1–100	0.65
100–1000	8.84
1000–10,000	6.23
>10,000	0.98
Total	16.70
4–300[a]	5.39
350–2000[b]	3.44

[a] Pore size range detrimental to frost resistance, according to Litvan [16].
[b] Pore size range effective for frost resistance, according to Litvan [17].

3.6. Pore structure characterization

Three samples were picked up from the concrete specimens after 90 days of wet curing, for testing them by means of the mercury intrusion technique. These samples consisted of only hydrated cement paste, after excluding both fibers and aggregate particles. The mean results are included in Table 6, where not only the total open porosity is reported but also the porosities corresponding to certain pore size ranges. In particular, attention was focused on those pore size ranges that were indicated by Litvan [16,17] as detrimental to frost resistance or effective for it. The results obtained showed a large amount of pores belonging to both detrimental and effective ranges; therefore, no useful information on frost resistance of concrete can be extrapolated.

3.7. Frost resistance

The frost resistance was measured according to the "Resistance of Concrete to Rapid Freezing and Thawing" Standard Test Method (ASTM C 666) following "Procedure B: Rapid Freezing in Air and Thawing in Water" on concrete cubic specimens (100 mm in size), wet cured for 90 days. Mass and dynamic elastic modulus of the concrete specimens were measured every 30 cycles in order to evaluate both the relative dynamic modulus (RDM) of elasticity and the percentage of mass change.

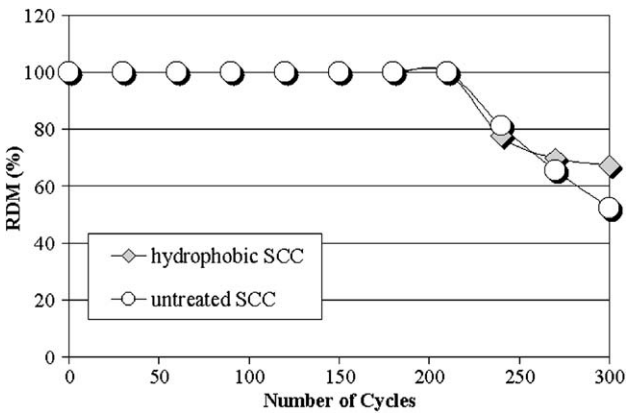

Fig. 6. RDM of elasticity of both untreated and hydrophobic concretes.

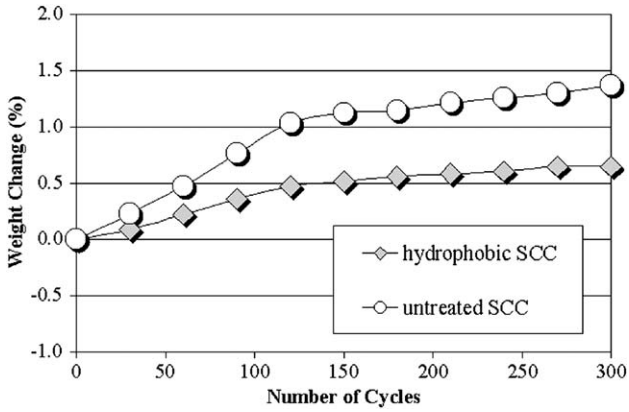

Fig. 7. Percentage of mass change of both untreated and hydrophobic concretes.

Six concrete specimens were tested; three of them were previously treated on their surface with an hydrophobic agent, such as a commercial product based on siloxane resins, in order to evaluate any decrease in water absorption for treated specimens and the consequent beneficial effect on vulnerability to freezing and thawing cycles. The results obtained up to 300 cycles showed that after 200 cycles, a significant trend towards low values of the RDM was detected in every case, especially for the untreated specimens (see Fig. 6). The durability factors result equal to 52 and 67, respectively, in the case of the absence and the presence of a hydrophobic surface, respectively, thus indicating a certain benefit related to the use of an hydrophobic agent. The mass change of the concrete specimens was also monitored, and the values obtained, expressed as a percentage with respect to the initial saturated condition, are reported in Fig. 7. The mass of the concrete specimens slightly increased up to 120 cycles (about 50% lower mass change was detected in the case of surface-treated specimens); subsequently, a fairly constant value was maintained. This may be explained by water absorption in the first period (less evident for hydrophobically treated specimens) and by the progressive depletion of this phenomenon; concrete scaling was never observed.

4. Conclusions

The concrete, which was prepared to manufacture thin precast elements for nonstructural applications, met both the self-compaction and mechanical requirements. The fiber addition proved to be very effective in counteracting drying shrinkage of self-compacting concrete, which is usually a great problem for this material, rich in powders and poor in the coarse aggregate fraction. Due to the very low porosity of its cementitious matrix, the rate of chloride ion diffusion was low. The resistance to freezing and thawing was

moderate and can be improved by the superficial application of a hydrophobic agent, which notoriously reduces water ingress into concrete. However, reminding of the type of applications to which the thin precast elements are devoted, self-compacting concrete durability is most satisfactory and it appears competitive with other materials in manufacturing these elements.

References

[1] M. Collepardi, A very close precursor of self-compacting concrete, in: V.M. Malhotra (Ed.), Suppl. Papers of the Third CANMET/ACI Int. Symp., San Francisco, ACI, Farmington Hills, MI, USA, 2001, pp. 431–450.

[2] M. Collepardi, R. Khurana, M. Valente, Construction of a dry dock using tremie superplasticized concrete, in: V.M. Malhotra (Ed.), Superplasticizers and Other Chemical Admixtures in Concrete, ACI SP-119, Farmington Hills, MI, USA, 2001, pp. 471–492.

[3] B. Van Khanh, D. Montgomery, Drying shrinkage of self-compacting concrete containing milled limestone, in: A. Skarendahl, O. Petersson (Eds.), 1st International RILEM Symposium on Self-Compacting Concrete, Stockholm, Sweden, RILEM Publications S.A.R.L., 1999, pp. 509–521.

[4] K.H. Khayat, Y. Roussel, Testing and performance of fiber-reinforced, self-consolidating concrete, in: A. Skarendahl, O. Petersson (Eds.), Self-Compacting Concrete, 1999, pp. 509–521, Stockholm, Sweden.

[5] P. Grouth, D. Nemegeer, The use of steel fibres in self-compacting concrete, in: A. Skarendahl, O. Petersson (Eds.), 1st International RILEM Symposium on Self-Compacting Concrete, Stockholm, Sweden, RILEM Publications S.A.R.L., 1999, pp. 497–507.

[6] S. Grünewald, J.C. Walraven, Self-compacting fibre-reinforced concrete, Heron 46 (3) (2001) 201–206.

[7] M. Ouchi, Y.A. Edamatsu, Simple evaluation method for interaction between coarse aggregate and mortar particles in self-compacting concrete, in: A. Skarendahl, O. Petersson (Eds.), 1st International RILEM Symposium on Self-Compacting Concrete, Stockholm, Sweden, RILEM Publications S.A.R.L., 1999, pp. 121–130.

[8] K.H. Khayat, Z. Guizani, Use of viscosity—modifying admixture to enhance stability of fluid concrete, ACI Mater. J. 94 (4) (1997) 332–340.

[9] F.M. Lea, The Chemistry of Cement and Concrete, 3rd ed., Edward Arnold (Publishers) Ltd, London, 1970, p. 408 (Table 69).

[10] J.-C. Chern, C.-H. Young, Compressive creep and shrinkage of steel fibre reinforced concrete, Cem. Concr. Compos. 11 (4) (1989) 205–214.

[11] A.A. Alekrish, S.H. Alsayed, Shrinkage of fiber and reinforced fiber concrete beams in hot–dry climate, Cem. Concr. Compos. 16 (4) (1994) 299–307.

[12] O. Kayali, M.N. Haque, B. Zhu, Drying shrinkage of fibre-reinforced lightweight aggregate concrete containing fly ash, Cem. Concr. Res. 29 (11) (1999) 1835–1840.

[13] H.A. Mesbah, F. Buyle-Bodin, Efficiency of polypropylene and metallic fibres on control of shrinkage and cracking of recycled aggregate mortars, Constr. Build. Mater. 13 (8) (1999) 439–447.

[14] M. Pauri, S. Monosi, I. Alverà, M. Collepardi, Assessment of free and bound chloride in concrete, Mater. Eng. 1 (2) (1990) 497–501.

[15] M. Collepardi, A. Marcialis, R. Turriziani, Penetration of chloride ions into cement pastes and concretes, J. Am. Ceram. Soc. 55 (10) (1972) 534–535.

[16] G.G. Litvan, Pore structure and frost susceptibility of building materials, in: S. Modrȳ, M. Svatā (Eds.), Pore Structure and Properties of Materials, Proceedings of the RILEM/IUPAC International Symposium, 18–21 September 1973, Prague, vol. II, Academia, Prague, Czechoslovakia, 1974, pp. F-17–F-30 (Final Report).

[17] G.G. Litvan, Air entrainment in the presence of superplasticizers, ACI J. 80 (4) (1983) 326–331.